Closed-Form Beamforming Aided Joint Optimization for Spectrum- and Energy-Efficient UAV-BS Networks

Ke Li†, Xu Zhu*, Yufei Jiang†, and Fu-Chun Zheng†
† School of Electronic and Information Engineering, Harbin Institute of Technology, Shenzhen, China
∗ Department of Electrical Engineering and Electronics, The University of Liverpool, Liverpool, UK
Emails: like2017@stu.hit.edu.cn, xuzhu@liverpool.ac.uk, jiangyufei@hit.edu.cn

***Abstract*— In this paper, we investigate a spectrum- and energy-efficient emergency wireless communication system with an unmanned aerial vehicle (UAV) mounted base station (BS). To the best of our knowledge, this is the first work to investigate joint optimization of three-dimensional (3D) beamforming (BF), power allocation (PA), user scheduling and UAV trajectory, to maximize the average spectrum efficiency (SE) while maintaining high energy efficiency (EE). Furthermore, a closed-form BF design in both angle- and power-domains is proposed for the first time for UAV-BS assisted wireless systems. Thanks to the closed-form solutions, a low-complexity iterative algorithm is proposed for joint optimization, which converges within only one or two iterations. Simulation results show that 3D BF plays a dominant role in the overall performance, and the proposed closed-form 3D BF design achieves near-optimal performance in terms of both EE and SE, while requiring much lower complexity than exhaustive search. The maximum UAV speed with respect to the optimal EE is also obtained.**

I. Introduction

Unmanned aerial vehicle (UAV) aided communications have been considered as an effective complementary to fifth generation (5G) networks [1]. Benefiting from flexible and fast deployment, low cost and the presence of the strong line of sight (LOS) link, UAV can act as an aerial base station (BS) to extend wireless coverage in emergency, for example, to resume the network connection of users in a post-disaster scenario [2][3] and to provide data offloading for terrestrial BS in cellular networks [4][5].

Rate maximization for UAV-assisted networks were investigated in [6] and [7]. With the objective of maximizing system sum rate, cooperative energy sharing among UAV-BSs was studied in [6]. In [7], the author investigated maximizing the lower bound of user achievable rate via joint design of user scheduling, power and UAV trajectory. However, the authors of both [6] and [7] have focused on maximizing the transmission rate without considering energy consumption.

Since limited battery constrains UAV mobility and hovering time, energy efficiency (EE) oriented design has attracted much attentions. Three-dimensional (3D) energy-efficient coverage was investigated in [8] via maximizing number of covered users with minimum transmission power, while UAV hovering energy consumption was ignored. In [9], EE was optimized for UAV-aided cellular offloading. In [10], spectrum efficiency (SE) and EE maximization was conducted for a UAV relaying system jointly designing time allocation of two hops and UAV trajectory. However, the power consumption model considered [9] and [10] is over-simplified, where transmission power is ignored. In [11], UAV trajectory and power optimization were investigated to maximize EE in sensing and data transmission scenario, taking transmission power into consideration. However, it assumed a rotary-wing UAV energy consumption model which cannot be applied to fixed-wing UAVs.

Beamforming (BF) is an effective technique for improving transmission rate [12]-[15]. BF of terrestrial BS was studied in [12] and later on BF design in UAV-aided systems was investigated in [13]-[15]. Joint BF and PA of UAV mobile relaying system was investigated in [13] and [14]. In [13], PA and BF for a UAV full-duplex relay are jointly optimized and the optimal closed-form two-dimensional (2D) BF solution was obtained. EE is maximized in [14] via optimizing PA, BF, trajectory radius and UAV speed. However, applying BF for single user [14] into multiuser case can result in severe interference. Besides, tilt optimization was ignored in both works. Joint 3D BF and UAV trajectory design of an UAV-enabled mobile relaying system was investigated in [15]. However, the BF tilt optimization in [15] operates in exhaustive manner, with tremendous complexity.

Motivated by the above open issues, in this paper, we investigate a UAV-BS assisted multiuser wireless system in an emergency scenario. A joint optimization scheme of low-complexity 3D BF, PA, user scheduling and UAV trajectory design is proposed to maximize the time-averaged sum achievable rate of all users, while maintaining high EE. The contributions of are summarized as follows.

1) To the best of our knowledge, this is the first work to investigate joint optimization of 3D BF, PA, user scheduling and UAV trajectory design in a UAV assisted wireless network. The nonconvex optimization problem formulated is solved in an iterative and computationally efficient manner, converging within only one or two iterations. Unlike the work in [7] which investigated joint optimization of user scheduling and UAV trajectory, we take an additional performance affecting factor of 3D BF into account. Simulation results show that 3D BF plays a dominant role in the overall performance, and

can nearly double the SE performance compared to the approach in [7].

2) Closed-form 3D BF and PA solutions are derived. To the best of our knowledge, this is the first closed-form 3D BF design in both angle- and power-domains for UAV-BS assisted wireless systems, while the previous closed-form BF solutions were derived in power-domain only [13][14], and most previous 3D BF designs require high complexity based searching [15]. The proposed 3D BF solution achieves near-optimal performance in terms of both EE and SE, while requiring much lower complexity than exhaustive search. It also significantly outperforms the searching based BF approach in [15].
3) We investigate both SE and EE for the UAV-BS assisted wireless network, with a practical power consumption model. Different from the propulsion power consumption only model in [9] and [10] and the fixed-wing UAV power consumption model in [11], our power consumption model is for rotary-wing UAVs and involves both communication and propulsion power consumptions. Compared to [16] which simply minimizes energy consumption, we maintain high EE and SE simultaneously. The maximum UAV speed with respect to the optimal EE is also obtained.

The rest of this paper is organized as follows. The system model and problem formulation are presented in Section II. The joint optimization algorithm and closed-form solutions are given in Section III. Complexity analysis and numerical results are presented in Sections IV and V, respectively. Section VI concludes the paper.

II. System Model and Problem Formulation

A. System Model

We consider a UAV-aided wireless communication system that comprises a UAV-BS equipped with M antennas and K users. Limited by the UAV size and on-board battery, it is assumed that $K >> M$. The UAV BS can not serve widely distributed users simultaneously on a fixed position. Cyclic time division multiple access (TDMA) is employed. Users are scheduled in group manner and are served at different slots, as illustrated in Fig. 1. The vertical distance between UAV and the users' plane is denoted as D. The flight time T_f is evenly divided into N time slots, and each time slot is allocated to the associated users. The number of slots N is sufficient large to guarantee that UAV location remains unchanged between two adjacent slots even with the maximum UAV speed V_{max}.

Without loss of generality, according to a 2D Cartesian coordinate system, users' horizontal coordinate is $\mathbf{w}_k = \begin{bmatrix} x_k & y_k \end{bmatrix}^T \in \mathbb{R}^{2\times1}, k \in \mathcal{K}$. The time-varying coordinate of UAV at slot n is denoted by $\mathbf{q}[n] = \begin{bmatrix} x[n] & y[n] \end{bmatrix}^T \in \mathbb{R}^{2\times1}$. Considering the cyclic flight and the maximum speed, the coordinate satisfies $\mathbf{q}[1] = \mathbf{q}[N]$ and $\|\mathbf{q}[n+1] - \mathbf{q}[n]\|^2 \le S_{\max}^2, n = 1, ..., N-1$, where $S_{\max} = \frac{V_{\max} T_f}{N}$ is the maximum distance that UAV can achieve between any two neighboring slots. The first constraint infers that UAV flies back to the initial location by the end of each period T_f to finish a cyclic flight. The second constraint implies that the UAV speed is bounded by a maximum speed limit.

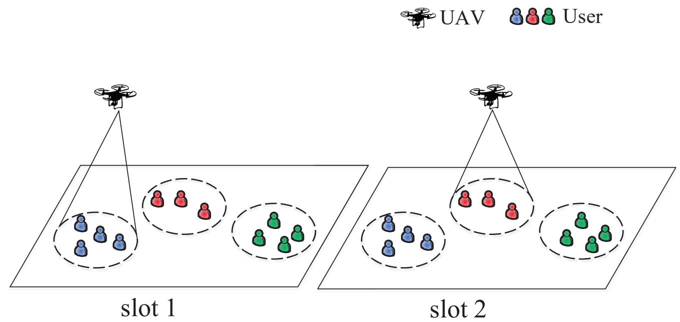

Fig. 1. A UAV enabled communication system

1) UAV Directional Antenna Pattern: We assume the number of radio frequency (RF) chains for UAV equals to the number of antennas M, therefore, each antenna element transmits different signals. For each scheduled user, we consider signals from one antenna as desired signal and treat signals from other antennas as interference.

UAV implements directional 3D antenna pattern and the beamwidth remains unchanged at a typical value proposed by 3rd Generation Partnership Project (3GPP) and thus the coverage of a single beam is finite. The UAV can change the beam coverage by adjusting its trajectory.

We focus on vertical BF, thus we assume the antenna pattern for horizontal region is omnidirectional and side-lobe levels for both planes are positive infinity. Hence, the vertical antenna gain with multiple antennas for user k is expressed as $\mathbf{g} = \begin{bmatrix} g_1 & g_2 & ... & g_M \end{bmatrix}^T$ where $g_k = 10^{\frac{-12\left(\frac{\theta_k}{\theta_{3dB}}\right)^2 + G_m}{10}}, k = 1, 2, ..., M$. θ_{3dB} denotes the half power beamwidth (HPBW) in vertical direction. G_m denotes the peak antenna gain. θ_k denotes the tilt between beam boresight and vertical direction for user k.

2) Air-Ground Channel Model: The received signals for user k is expressed as $y_k = \mathbf{h}^T\mathbf{x} + n_k$ where $\mathbf{h} = \begin{bmatrix} h_1 & h_2 & ... & h_M \end{bmatrix}^T$ is the channel vector for user k and $\mathbf{x} = \begin{bmatrix} \sqrt{g_1}x_1 & \sqrt{g_2}x_2 & ... & \sqrt{g_M}x_M \end{bmatrix}^T$ is the signal transmitted from the UAV. $x_i, i = 1, 2, ..., M$ denotes the data transmitted from i-th antenna element. n_k denotes the additive white Gaussian noise (AWGN) for user k.

We assume that dominant LOS component exists in the UAV-users links, and thus the channel quality depends on the distance between the UAV and users. Furthermore, we assume that the doppler shift caused by UAV mobility is well compensated. We assume that k-th antenna element transmits the desired signal for user k and the distances between k-th antenna element and user k is denoted by d_k. Hence, the channel gain from user k to the k-th antenna element of UAV can be expressed by

$$h_k^g = \beta_0 d_k^{-2} = \frac{\beta_0}{D^2 + \left\| \mathbf{q}\left[n\right] - \mathbf{w}_k \right\|^2}, \forall n \tag{1}$$

where β_0 denotes channel gain at reference distance $d_0 = 1$ m. The overall transmission power of UAV is bounded by maximum transmission power budget at each slot as $\sum\limits_{i=1}^{M} p_i \leq P_{\max}, \forall n$ where p_i is the transmission power of antenna element i satisfying $p_i = E\left[x_i^2\right]$ and $P_{\max}$ is the maximum transmission power of UAV at each slot. For tractability concern, we assume that the number of users scheduled at one slot is no more than 2.

Hence, the achievable rate for user k can be expressed as

$$R_k = \log_2\left(1 + \gamma_k\right) \tag{2}$$

where $\gamma_k = \frac{g_k h_k^g p_k}{\sum\limits_{m=1, m \neq k}^{M} g_m h_m^g p_m + \sigma^2}$ is the signal to interference and noise ratio (SINR) of user k and σ^2 is the average power of AWGN at the receiver.

B. Problem Formulation

We use a user scheduling indicator α_k to indicate that user k is scheduled if $\alpha_k = 1$, otherwise $\alpha_k = 0$. We assume that each user is scheduled at least once during the whole flight time to ensure user fairness. Hence, the user scheduling indicator should satisfy $\sum\limits_{n=1}^{N} \alpha_k \leq 1, \forall k$ and $\alpha_k \in \left\{0, 1\right\}, \forall k, n$. Furthermore, the associated users set at slot n is denoted by $S_n = \left\{ k \middle| \alpha_k = 1 \right\}, \forall n$.

System SE is expressed as

$$\eta_{SE} = \frac{1}{N} \sum_{n=1}^{N} \sum_{k=1}^{K} \alpha_k R_k \tag{3}$$

In EE evaluation, we consider both the transmission power $P_{\max}$ and the propulsion power $P\left(V\right)$ which is a function of UAV flying speed V [16]. EE is expressed as

$$\eta_{EE} = \frac{B}{N} \sum_{n=1}^{N} \sum_{k=1}^{K} \frac{\alpha_k R_k}{P\left(V\right) + P_{\max}} \tag{4}$$

where B denotes the total bandwidth.

As shown in [16], the propulsion power has minor variations at a relatively low UAV speed ($V < 14$ m/s). This implies that with a given transmission power which is normally less than the propulsion power, high EE can be maintained by maximizing SE.

Let $\mathbf{A} = \left\{\alpha_k, \forall k, n\right\}, \mathbf{Q} = \left\{\mathbf{q}\left[n\right], \forall n\right\}, \mathbf{P} = \left\{p_k, \forall k, n\right\}, \boldsymbol{\theta} = \left\{\theta_k, \forall k\right\}$ denote the variables of user scheduling, UAV trajectory, PA and BF tilt, respectively. The optimization problem is formulated as

$$(P0) \max_{\mathbf{A}, \mathbf{P}, \boldsymbol{\theta}, \mathbf{Q}} \frac{1}{N} \sum_{n=1}^{N} \sum_{k=1}^{K} \alpha_k R_k \tag{5a}$$

$$\text{s.t.} \quad C_1 : \alpha_k \in \left\{0, 1\right\}, \forall k, n \tag{5b}$$

$$C_2 : \sum_{n=1}^{N} \alpha_k \leq 1, \forall k \tag{5c}$$

$$C_3 : \left\| \mathbf{q}\left[n+1\right] - \mathbf{q}\left[n\right] \right\|^2 \leq S_{\max}^2, n = 1, ..., N-1 \tag{5d}$$

$$C_4 : \mathbf{q}\left[1\right] = \mathbf{q}\left[N\right] \tag{5e}$$

$$C_5 : \theta_{\min} \leq \theta_k \leq \theta_{\max}, \forall k \tag{5f}$$

$$C_6 : \sum_{k \in \mathcal{S}_n} p_k \leq P_{\max}, \forall n \tag{5g}$$

where C_1 and C_2 are the user scheduling constraints; C_3 denotes the maximum speed constraint while C_4 ensures a periodic flight; C_5 confines the BF tilt; C_6 denotes the transmission power budget.

III. 3D BF Aided Joint Optimization

To make problem $(P0)$ more tractable, we first relax binary variables in C_3 into continuous variables , which serves as an upper bound of the original problem $(P0)$. Hence, we have problem $(P1)$ expressed as

$$\begin{aligned} &(P1) \max_{\mathbf{A}, \mathbf{P}, \boldsymbol{\theta}, \mathbf{Q}} \tfrac{1}{N} \sum_{n=1}^{N} \sum_{k=1}^{K} \alpha_k R_k \\ &\text{s.t.} \quad C_1 : 0 \leq \alpha_k \leq 1, \forall k, n \ and \ C_2 - C_6 \end{aligned} \tag{6}$$

Problem $(P1)$ is still nonconvex. To tackle the nonconvex problem $(P1)$, we propose an iterative algorithm by applying block coordinate descent and successive convex approximation to optimize user scheduling $\mathbf{A}$, PA $\mathbf{P}$, BF tilt $\boldsymbol{\theta}$, UAV trajectory $\mathbf{Q}$ in an iterative manner.

The joint optimization algorithm is operated as follows. First, for given $\mathbf{P}$, $\mathbf{Q}$ and $\boldsymbol{\theta}$, $\mathbf{A}$ is optimized by solving a linear programming (LP) problem. Second, Given $\mathbf{A}$, $\mathbf{Q}$ and $\boldsymbol{\theta}$, we derive the closed-form solution for $\mathbf{P}$. Third, given $\mathbf{A}$, $\mathbf{Q}$ and $\boldsymbol{\theta}$, the closed-form solution for $\boldsymbol{\theta}$ is derived. Finally, given $\mathbf{A}$, $\mathbf{P}$ and $\boldsymbol{\theta}$, we optimize UAV trajectory $\mathbf{Q}$ via successive convex approximation technique.

A. User Scheduling Optimization

For any given UAV trajectory, PA and BF tilt $\left\{\mathbf{Q}, \mathbf{P}, \boldsymbol{\theta}\right\}$, user scheduling issue can be optimized by solving the following problem.

$$\begin{aligned} &(P1.1) \max_{\mathbf{A}} \tfrac{1}{N} \sum_{n=1}^{N} \sum_{k=1}^{K} R_k \\ &\text{s.t.} \quad C_1 \ and \ C_2 \end{aligned} \tag{7}$$

Since problem $(P1.1)$ is a standard LP problem, it can be solved via convex optimization tool such as CVX.

B. Power Allocation

For any given user scheduling, UAV trajectory and BF tilt $\{\mathbf{A}, \mathbf{Q}, \boldsymbol{\theta}\}$, the subproblem of PA is presented as follows.

$$\begin{aligned} &(P1.2)\max_{\mathbf{P}} \tfrac{1}{N}\sum_{n=1}^{N}\sum_{k\in S_n} R_k \\ &\text{s.t.} \quad C_6 \end{aligned} \tag{8}$$

Note that problem $(P1.2)$ is still nonconvex due to nonconvex form in the objective function. To tackle the problem, we introduce an auxiliary variable I to confine the intra-beam interference as $C_7: \sum_{m\in S_n, m\neq k} g_m h_m^g p_m < I, \forall k$.

By adding C_7, problem $(P1.2)$ is a convex optimization problem in general and can be solved via Lagrange dual method and Karush–Kuhn–Tucker (KKT) conditions. The Lagrange dual function and KKT conditions are expressed as

$$\begin{aligned} L(\mathbf{P},\lambda) = &-\frac{1}{N}\sum_{n=1}^{N}\sum_{k\in S_n} R_k + \lambda_0\left(\sum_{k\in S_n} p_k - P_{\max}\right) \\ &+ \mu_0\left(\sum_{m\in S_n, m\neq k} g_m h_m^g p_m - I\right), \forall n \end{aligned} \tag{9}$$

$$\frac{\partial L}{\partial p_k} = -\frac{1}{1+\gamma_k}\cdot\frac{\partial \gamma_k}{\partial p_k} + \lambda_0 = 0, \forall n \tag{10a}$$

$$\lambda_0\left(\sum_{k\in S_n} p_k - P_{\max}\right) = 0, \forall n \tag{10b}$$

$$\mu_0\left(\sum_{m\in S_n, m\neq k} g_m h_m^g p_m - I\right) = 0, \forall n \tag{10c}$$

Hence, we can obtain the closed-form solution of PA as $p_k = \left(\frac{1}{\lambda_0} - \frac{I+\sigma^2}{g_k h_k^g}\right)^{\dagger}$ where $(\cdot)^{\dagger}$ returns the maximum between the argument and zero and $\lambda_0 = \frac{\|S_n\|}{P_{\max} + \sum_{k\in S_n}\frac{I+\sigma^2}{g_k h_k^g}}$.

C. Beamforming Tilt Optimization

For given user scheduling, UAV trajectory and PA $\{\mathbf{A}, \mathbf{Q}, \mathbf{P}\}$, BF tilt can be optimized by solving problem $(P1.3)$ expressed in the following.

$$\begin{aligned} &(P1.3)\max_{\boldsymbol{\theta}} \tfrac{1}{N}\sum_{n=1}^{N}\sum_{k\in S_n} R_k \\ &\text{s.t.} \quad C_5 \end{aligned} \tag{11}$$

Evidently, since logarithmic form exists in R_k, the following equation always holds.

$$\frac{1}{\|S_n\|}\sum_{k\in S_n}\log_2(1+\gamma_k) < \frac{1}{\|S_n\|}\sum_{k\in S_n}(1+\gamma_k) \tag{12}$$

Hence, we rewrite the problem $(P1.3)$ into an equivalent form as follows.

$$\begin{aligned} &(P1.3.1)\max_{\boldsymbol{\theta}} \ \tfrac{1}{N}\sum_{n=1}^{N}\sum_{k\in S_n}\gamma_k \\ &\text{s.t.} \quad C_5 \end{aligned} \tag{13}$$

Note that the solution of problem $(P1.3)$ is upper bounded by the counterpart of $(P1.3.1)$. We use two-user case as an illustration, namely, the user assigned to the same group is 2. Hence, the objective function of $(P1.3.1)$ is rewritten as $\frac{1}{N}\sum_{n=1}^{N}\left(\frac{g_1F_1}{g_2F_2+\sigma^2} + \frac{g_2F_2}{g_1F_1+\sigma^2}\right)$ where $F_k = h_k^g p_k, k = 1, 2$. The objective function for problem $(P1.3.1)$ is strictly quasi-concave with respect to $\boldsymbol{\theta}$. We note that $g_kF_k \gg \sigma^2, k = 1, 2$ and $g_1 \approx g_2$. Hence, we can get the closed-form solution which is shown in the following via first-order derivative of the objective function of $(P1.3.1)$.

$$\theta_k^* = \frac{1}{\|S_n\|}\sum_{m\in S_n}\theta_m, k = 1, 2 \tag{14}$$

D. UAV Trajectory Design

For any given user scheduling, PA and BF tilt $\{\mathbf{A}, \mathbf{P}, \boldsymbol{\theta}\}$, the UAV trajectory design is formulated as subproblem $(P1.4)$.

$$\begin{aligned} &(P1.4)\max_{\mathbf{Q}} \tfrac{1}{N}\sum_{n=1}^{N}\sum_{k\in S_n} R_k \\ &\text{s.t.} \quad C_3 \ and \ C_4 \end{aligned} \tag{15}$$

Problem $(P1.4)$ is a nonconvex problem and the objective function can be rewritten as $\frac{1}{N}\sum_{n=1}^{N}\sum_{k\in S_n}\left(\hat{R}_k - \tilde{R}_k\right)$ where $\hat{R}_k = \log_2\left(\sum_{m\in S_n}\frac{\beta_0 g_m p_m}{D^2+\|\mathbf{q}[n]-\mathbf{w}_m\|^2} + \sigma^2\right)$ and $\tilde{R}_k = \log_2\left(\sum_{\substack{m\in S_n \\ m\neq k}}\frac{\beta_0 g_m p_m}{D^2+\|\mathbf{q}[\mathbf{n}]-\mathbf{w}_m\|^2} + \sigma^2\right)$. However, it is still nonconvex. Thus, we adopt successive convex approximation technique to substitute the original function with an approximated version at a given point in each iteration. We define $\mathbf{Q}^r = \{\mathbf{q}^r[n], \forall n\}$ as the given trajectory in r-th iteration. We utilize first-order Taylor expansion as a lower bound to approximate the original function. Given local point $\mathbf{Q}^r$ in r-th iteration, $\hat{R}_k$ is bounded by $\hat{R}_k^{lb}$. $\hat{R}_k^{lb}$ is omitted here due to space limitation and can be found in [7]. With any given local point $\mathbf{Q}^r$ as well as lower bound, we obtain the following optimization problem as

$$\begin{aligned} &(P1.4.1)\max_{\mathbf{Q}} \ \tfrac{1}{N}\sum_{n=1}^{N}\sum_{k\in S_n}\left(\hat{R}_k^{lb} - \tilde{R}_k\right) \\ &\text{s.t.} \quad C_3 \ and \ C_4 \end{aligned} \tag{16}$$

Hence, problem $(P1.4.1)$ is convex and can be solved via CVX.

E. Overall Algorithm For 3D BF Aided Joint Optimization

Now we are able to devise the whole algorithm as follows. First we optimize $\mathbf{A}$ with fixed $\mathbf{P}, \mathbf{Q}$ and $\boldsymbol{\theta}$. Then, we turn to design $\mathbf{P}$ for given $\mathbf{A}, \mathbf{Q}$ and $\boldsymbol{\theta}$. Next, we obtain $\boldsymbol{\theta}$ for given $\mathbf{A}, \mathbf{P}$ and $\mathbf{Q}$. Finally, we optimize $\mathbf{Q}$ with given $\mathbf{A}, \mathbf{P}$ and $\boldsymbol{\theta}$. The detailed algorithm is summarized in Algorithm 1.

Algorithm 1 Proposed iterative algorithm

1: Initialize $\mathbf{P}^0, \boldsymbol{\theta}^0$ and $\mathbf{Q}^0$. Let iteration index $r = 0$.
2: **repeat**
3: Solve problem $(P1.1)$ for given $\mathbf{P}^r, \mathbf{Q}^r$ and $\boldsymbol{\theta}^r$, and denote the optimal solution as $\mathbf{A}^{r+1}$.
4: Solve problem $(P1.2)$ for given $\mathbf{A}^{r+1}, \boldsymbol{\theta}^r$ and $\mathbf{Q}^r$, and denote the optimal solution as $\mathbf{P}^{r+1}$.
5: Solve problem $(P1.3)$ for given $\mathbf{A}^{r+1}, \mathbf{P}^{r+1}$ and $\mathbf{Q}^r$, and denote the optimal solution as $\boldsymbol{\theta}^{r+1}$.
6: Solve problem $(P1.4)$ for given $\mathbf{A}^{r+1}, \mathbf{P}^{r+1}$ and $\boldsymbol{\theta}^{r+1}$, and denote the optimal solution as $\mathbf{Q}^{r+1}$.
7: Update $r = r + 1$.
8: **until** The fractional increase of the objective value is below a threshold $\epsilon > 0$.

IV. Complexity Analysis

In this section, we present the complexity analysis for the proposed BF method and the exhaustive search based optimal BF is selected as benchmark. For the two different schemes, analytical and numerical complexity are presented. Thanks to the closed-form solution, the proposed BF achieves much lower complexity than optimal BF by exhaustive search. The complexity reduction is N times. When the number of flight time slots is $N = 200$, a 200-fold complexity reduction is achieved. We note that the complexity for the optimal BF is determined by step length of search. Detailed analytical and numerical complexity are illustrated in TABLE I.

TABLE I
Complexity Analysis for different BF schemes(N–Number of time slots)

Method	Analytical	Numerical ($N = 200$)
Closed-form 3D BF	$\mathcal{O}(N)$	200
Optimal BF	$\mathcal{O}(N^2)$	40000

V. Simulation Results

In this section, we present some numerical results to demonstrate the effectiveness of the proposed algorithm. We have $K = 6$ users and the bandwidth is set as $B = 1$ MHz. Users are distributed in a 100×100 square region. The HPBW is set as $\theta_{3dB} = 6^\circ$ [12]. The distance between UAV and the users' plane is fixed as $D = 100$ m and the average noise power is assumed to be $\sigma^2 = -110$ dBm [7]. The number of antennas is $M = 2$. The channel power gain is $\beta_0 = -80$ dB [17]. The threshold ϵ in Algorithm 1 is set as 10^{-2}. Each second of flight time T_f consists of 10 equal sub-slots. The number of time slots is $N = 10T_f$.

The EE performance of different BF schemes are presented in Fig. 2. The proposed BF solution achieves near-optimal performance in terms of both EE and SE. It also significantly outperforms the searching based BF approach in [15]. It can be observed that EE first increases and then decreases with the increase of the UAV speed. Since with low propulsion power consumption in low speed limit range, UAV prefers to move fast and hover above users to enjoy better communication link, thus boosts EE. However, high mobility leads to minor rate increase if UAV is able to stay stationary above users for sufficient long time and the power consumption rises, thus results in EE reduction. The maximum EE is achieved at a relatively low maximum UAV speed of approximately $V_{\max} = 7$ m/s.

In Fig. 3, we present the results of SE performance under different strategies. It is observed that BF schemes outperform the BF-excluded scheme, proving the effectiveness of BF design. Compared with optimal BF, the proposed BF achieves near-optimal performance and much lower complexity. The proposed closed-form 3D BF also achieves much higher SE than the BF design in [15].

In Fig. 4, the convergence behaviour of the proposed algorithm with closed-form 3D BF is presented, where at most 2 iterations are required for convergence.

In Fig. 5, we illustrate the optimized trajectory obtained by proposed iterative algorithm under different flight time T_f. With a large value of T_f, the UAV has sufficient time to move closer to the users. Besides, if the flight time is sufficiently large, *i.e.*, $T_f = 60$ s, UAV prefers to stay stationary at some locations to enjoy the best channel rather than keep enlarging its flying route.

VI. Conclusion

In this paper, we have investigated joint optimization for spectrum- and energy-efficient UAV-BS assisted wireless networks. A closed-form 3D BF design has been proposed, which not only presents near-optimal performance in terms of EE and SE, but also achieves a 200-fold complexity reduction with a flying time of 20 s, compared to exhaustive search. It also achieves nearly doubled EE and SE performances compared to the BF approach in [15]. We have also investigated EE with practical power consumption model for rotary-wing UAVs. The maximum of EE can be obtained at a relatively low maximum UAV speed of 7 m/s, implying the green feature of the system.

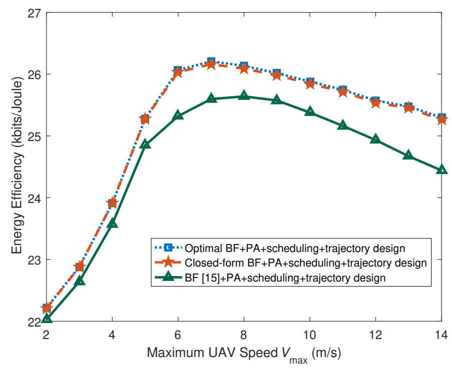

Fig. 2. Impact of maximum UAV speed $V_{\max}$ on EE with flight time $T_f = 20$ s and UAV transmission power $P_{\max} = 100$ mW.

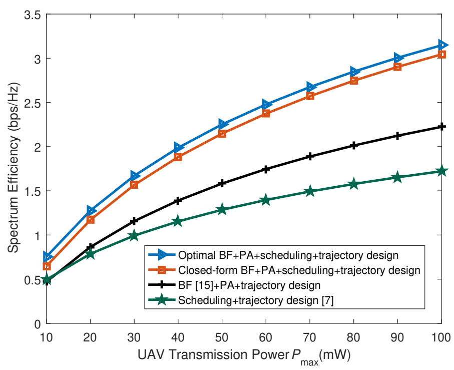

Fig. 3. Impact of UAV transmission power on SE with flight time $T_f = 20$ s and maximum UAV speed $V_{\max} = 7$ m/s

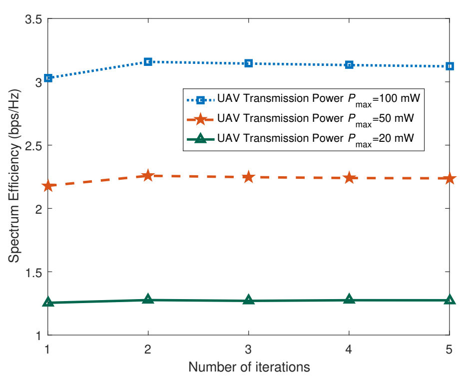

Fig. 4. Convergence behavior of the closed-form 3D BF aided optimization algorithm with flight time $T_f = 20$ s and maximum UAV speed $V_{\max} = 7$ m/s

REFERENCES

[1] Y. Zeng et al., "Wireless Communications with Unmanned Aerial Vehicles: Opportunities and Challenges," *IEEE Commun. Mag.*, vol. 54, no. 5, pp. 36-42, May 2016.

[2] N. Zhao et al., "UAV-Assisted Emergency Networks in Disasters," *IEEE Wireless Commun.*, vol. 26, no. 1, pp. 45-51, Feb. 2019.

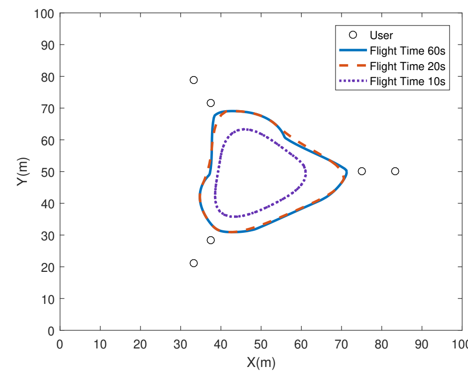

Fig. 5. Impact of flight time on UAV trajectory with maximum UAV speed $V_{\max} = 7$ m/s

[3] F. Cheng at el., "Learning-Based User Association in Multi-UAV Emergency Networks with Ground D2D," in *IEEE ICC Workshops*, Shanghai, China, 2019, pp. 1-5.

[4] N. Zhao et al., "Caching UAV Assisted Secure Transmission in Hyper-Dense Networks Based on Interference Alignment," *IEEE Wireless Commun.*, vol. 66, no. 5, pp. 2281-2294, May 2018.

[5] N. Zhao et al., "Caching Unmanned Aerial Vehicle-Enabled Small-Cell Networks: Employing Energy-Efficient Methods That Store and Retrieve Popular Content,"*IEEE Veh. Technol. Mag.*, vol. 14, no. 1, pp. 71-79, Mar. 2019.

[6] Y. Wang et al., "Dynamically Connectable UAV Base Stations with Cooperative Energy Sharing," in *Proc. IEEE Globecom 2018*, Abu Dhabi, United Arab Emirates, 2018, pp. 1-6.

[7] Q. Wu et al., "Joint Trajectory and Communication Design for UAV-Enabled Multiple Access," in *Proc. IEEE Globecom 2017*, Singapore, 2017, pp. 1-6.

[8] M. Alzenad et al., "3-D Placement of an Unmanned Aerial Vehicle Base Station (UAV-BS) for Energy-Efficient Maximal Coverage," *IEEE Wireless Commun. Lett.*, vol. 6, no. 4, pp. 434-437, Aug. 2017.

[9] M. Hua et al., "Energy-Efficient Optimization for UAV-aided Cellular Offloading," *IEEE Wireless Commun. Lett.*, pp. 1-1, 2019 (Early-Access).

[10] J. Zhang et al., "Spectrum and Energy Efficiency Maximization in UAV-Enabled Mobile Relaying," in *Proc. IEEE ICC 2017*, Paris, 2017, pp. 1-6.

[11] S. Zhang et al., "Joint Trajectory and Power Optimization for UAV Sensing Over Cellular Networks," *IEEE Commun. Lett.*, vol. 22, no. 11, pp. 2382-2385, Nov. 2018.

[12] N. Seifi et al., "Adaptive Multicell 3-D Beamforming in Multiantenna Cellular Networks," *IEEE Trans. Veh. Technol.*, vol. 65, no. 8, pp. 6217-6231, Aug. 2016.

[13] Q. Song et al, "Joint Beamforming and Power Allocation for UAV-Enabled Full-Duplex Relay," *IEEE Trans. Veh. Technol.*, vol. 68, no. 2, pp. 1657-1671, Feb. 2019.

[14] Q. Song et al., "Energy-Efficient Multi-Antenna UAV-Enabled Mobile Relay," *China Commun.*, vol. 15, no. 5, pp. 41-50, May 2018.

[15] Q. Yuan et al., "Joint 3D Beamforming and Trajectory Design for UAV-Enabled Mobile Relaying System," *IEEE Access*, vol. 7, pp. 26488-26496, 2019.

[16] Y. Zeng et al., "Energy Minimization for Wireless Communication With Rotary-Wing UAV," *IEEE Trans. Wireless Commun.*, vol. 18, no. 4, pp. 2329-2345, Apr. 2019.

[17] G. Zhang et al, "Securing UAV Communications via Joint Trajectory and Power Control," *IEEE Trans. Wireless Commun.*, vol. 18, no. 2, pp. 1376-1389, Feb. 2019.